

Structure evolution and entropy change of temperature and magnetic field induced magneto-structural transition in $\text{Mn}_{1.1}\text{Fe}_{0.9}\text{P}_{0.76}\text{Ge}_{0.24}$

Ming Yue, Danmin Liu, Qingzhen Huang, Tong Wang, Fengxia Hu, Jingbo Li, Guanghui Rao, Baogen Shen, Jeffery W. Lynn, and Jiuxing Zhang

Citation: *Journal of Applied Physics* **113**, 043925 (2013); doi: 10.1063/1.4788803

View online: <http://dx.doi.org/10.1063/1.4788803>

View Table of Contents: <http://scitation.aip.org/content/aip/journal/jap/113/4?ver=pdfcov>

Published by the [AIP Publishing](#)



Re-register for Table of Content Alerts

Create a profile.



Sign up today!



Structure evolution and entropy change of temperature and magnetic field induced magneto-structural transition in $\text{Mn}_{1.1}\text{Fe}_{0.9}\text{P}_{0.76}\text{Ge}_{0.24}$

Ming Yue,^{1,a)} Danmin Liu,² Qingzhen Huang,³ Tong Wang,⁴ Fengxia Hu,⁴ Jingbo Li,⁴ Guanghui Rao,⁴ Baogen Shen,⁴ Jeffery W. Lynn,^{3,b)} and Jiuxing Zhang¹

¹Key Laboratory of Advanced Functional Materials, Ministry of Education, College of Materials Science and Engineering, Beijing University of Technology, Beijing 100124, People's Republic of China

²Institute of Microstructure and Property of Advanced Materials, Beijing University of Technology, Beijing 100124, People's Republic of China

³NIST Center for Neutron Research, National Institute of Standards and Technology, Maryland 20899, USA

⁴Beijing National Laboratory for Condensed Matter Physics, Institute of Physics, Chinese Academy of Sciences, Beijing 100190, China

(Received 25 October 2012; accepted 4 January 2013; published online 30 January 2013)

The compound $\text{Mn}_{1.1}\text{Fe}_{0.9}\text{P}_{0.76}\text{Ge}_{0.24}$ has been studied using neutron powder diffraction (NPD), differential scanning calorimeter (DSC), and magnetic measurements, in order to clarify the nature of the magnetic and structural transition and measure the associated entropy change (ΔS). The strongly first order transition occurs from a paramagnetic (PM) to a ferromagnetic (FM) phase and can be induced either by temperature or by an applied magnetic field. Our investigations indicate that the two processes exhibit identical evolutions regarding the crystal and magnetic structures, indicating they should have the same entropy change. We, therefore, conclude that the ΔS_{DSC} obtained by the DSC method (where the transition is temperature induced) is valid also for the magnetically induced transition, thus avoiding uncertainties connected with the magnetic measurements. We have obtained the $\Delta S_{DSC} = 33.8 \text{ J/kg} \cdot \text{K}$ for this sample upon cooling, which would increase to $42.7 \text{ J/kg} \cdot \text{K}$ for a impurity-free and completely homogeneous sample. For comparison, the magnetic entropy changes (ΔS_M) induced by magnetic field and calculated using the Maxwell relation yields a $\Delta S_M = 46.5 \text{ J/kg} \cdot \text{K}$, 38% higher than ΔS_{DSC} . These entropy results are compared and discussed. © 2013 American Institute of Physics. [<http://dx.doi.org/10.1063/1.4788803>]

I. INTRODUCTION

In recent years magnetic refrigeration based on the magneto-caloric effect (MCE) has drawn tremendous attention due to its high energy efficiency, environmental amity, and hence good potential as an alternative to vapor-compression techniques around room temperature.¹ As a result, materials with large MCE at ambient temperatures such as $\text{Gd}_5(\text{Si}_x\text{Ge}_{1-x})_4$, $\text{La}(\text{Fe}_{1-x}\text{Si}_x)_{13}$, $\text{MnFe}(\text{P}_{1-x}\text{As}_x)$, and NiMnGa have been underdevelopment and broadly investigated.²⁻⁵ More recently, the $\text{MnFe}(\text{P}_{1-x}\text{Ge}_x)$ compound, a derivative of $\text{MnFe}(\text{P}_{1-x}\text{As}_x)$, has become a more promising candidate for commercial application in magnetic refrigeration not only for its giant MCE and tunable Curie temperature (T_C), but also for its competitive advantages such as abundant raw materials, low fabrication costs, and environmental friendly composition. It is now well accepted that the mechanism behind the giant MCE in MnFePGe compounds involves a magnetic transformation between the paramagnetic (PM) and ferromagnetic (FM) phase combined with significant anisotropic structural variations.⁶⁻¹⁷ It has been shown by the neutron diffraction experiments on the $\text{Mn}_{1.1}\text{Fe}_{0.9}\text{P}_{0.8}\text{Ge}_{0.2}$ compound that such variations can be induced by an applied magnetic field or by temperature, and that the formation of the FM phase is associated with an

expansion of the hexagonal unit cell in the direction of the a and b axes and with a contraction of the c axis.¹⁵ Up to now, improvements in enhancing the giant MCE and reducing the thermal and magnetic hysteresis have been studied by changing the composition, structure, and preparation methods of the compound.⁶⁻¹⁷ The large discrepancies among the magnetic entropy changes in samples with identical nominal composition reported by different MCE researchers and even the method of evaluation of the MCE property are still under dispute.

The latter problem arises mainly from the method to obtain the magnetic entropy change (ΔS_M), the key parameter necessary to evaluate the MCE of magnetic refrigerant materials. This quantity can be calculated by two indirect methods. One popular way is to obtain the ΔS_M from the isothermal magnetization curves with either the Maxwell¹⁸ or Clausius-Clapeyron relation.¹⁹ Another more reliable way is to derive ΔS_M from heat capacity measurements under different magnetic fields. However, the conventional methods of measuring heat capacity are time consuming and not suitable for materials with first order transition since a heat input does not necessarily lead to a temperature modification in the sample due to the latent heat. A reliable and fast method to obtain ΔS is the differential scanning calorimeter (DSC) which measures the heat flux, while the temperature of the calorimeter is continuously changed, and with proper integration of the calibrated signal the latent heat of the transition can be obtained. Therefore, DSC is particularly suited in the case of first order phase transitions since it yields both

^{a)}Author to whom correspondence should be addressed. Electronic mail: yueming@bjut.edu.cn. Tel.: +861067391760. Fax: +861067391760.

^{b)}Author to whom correspondence should be addressed. Electronic mail: Jeff.Lynn@nist.gov. Tel.: +13019756246. Fax: +13019759847.

the latent heat and the entropy changes associated with the transitions. In addition, these measurements directly provide both the magnetic and the structural contributions to ΔS . Unfortunately, DSC instruments where the magnetic field can be changed are not commercially available.^{20–22}

The entropy changes associated with the magnetically induced PM-FM transition have been extensively studied as function of field strength and Ge content. However, the effects of magnetic field and of the compositional heterogeneities in the sample on the PM phase that remains untransformed have been seldom considered. In our recent studies,^{15,17} we found that properly annealed samples of $\text{Mn}_{1.1}\text{Fe}_{0.9}\text{P}_{0.8}\text{Ge}_{0.2}$ exhibit a higher T_C , a larger MCE, and a narrower width of the PM-FM phase coexistence than those sintered, due to a more homogeneous composition and microstructure induced in the sample by the annealing process (see also Ref. 14). All of the above studies indicate that the structural and compositional homogeneities play an important role in tuning and optimizing the MCE. Since different preparation techniques were used in various studies, samples of MnFePGe may have quite different structural and compositional homogeneities and different amounts of untransformed PM phase even when they have identical nominal compositions. Such problems remind us that we need to normalize our ΔS values considering the impurity content and untransformed PM phase before making comparisons, and, more importantly, we need to explore more effective ways to improve the homogeneity and the MCE in this class of materials.

In our previous studies of the PM-FM transition in the compound of composition $\text{Mn}_{1.1}\text{Fe}_{0.9}\text{P}_{0.8}\text{Ge}_{0.2}$, we found that the effect of temperature on the nature of the transition is basically equivalent to that of an applied magnetic field.^{12,15} This result suggests that the DSC measurements are basically the proper way to determine the entropy change as well as other thermodynamic quantities of the materials under study. The aim of the present paper is to establish a quantitative relationship between ΔS_M obtained from magnetic measurements and ΔS derived from DSC experiments.

II. EXPERIMENTAL PROCEDURES

A polycrystalline sample of $\text{Mn}_{1.1}\text{Fe}_{0.9}\text{P}_{0.76}\text{Ge}_{0.24}$ was prepared by the ball milling and subsequent spark plasma sintering method as described in previous work.¹² The composition quoted throughout is that obtained from the diffraction refinements rather than nominal composition. Detailed neutron diffraction measurements as a function of temperature and applied magnetic field were carried out at NCNR on the high-intensity BT9 triple axis spectrometer. A pyrolytic graphite (PG) (002) monochromator was employed to provide neutrons of wavelength 2.36 Å, and a PG filter was used to suppress higher-order wavelength contaminations. Coarse 40' full-width-at-half-maximum (FWHM) collimation was employed, and no energy analyzer was used in these measurements. High resolution powder diffraction data were collected on the BT-1 neutron powder diffractometer using monochromatic neutrons of wavelength 1.5403 Å produced by a Cu (311) monochromator. Söller collimations before

and after the monochromator and after the sample were 15', 20', and 7' FWHM), respectively. Data were collected in the 2θ range of 3° to 168° with a step size of 0.05° for various temperatures. Magnetic measurements were carried out with a vertical field 7 T superconducting magnet. Refinements of the nuclear and magnetic structures were carried out using neutron powder diffraction data and the program GSAS. Uncertainties quoted represent one standard deviation.

A TA Instrument DSC Q200 equipped with a refrigerated cooling system (RCS) was used for all the calorimetric measurements. Nitrogen gas with a flow rate of 50 ml/min was used to purge the cell. The temperature and the enthalpy were calibrated using Indium as a standard. Samples of about 20 mg were investigated by heating and cooling at 60 K/h and 300 K/h between 190 K and 320 K. The mass heat capacity C_p of the sample was obtained by the standard procedure. Then the entropy of the magnetic transition was evaluated by numerical integration of

$$\Delta S = S_{T_2} - S_{T_1} = \int_{T_1}^{T_2} \frac{C_p}{T} dT.$$

The temperature and field dependence of the magnetization were measured in a quantum design SQUID. The magnetic entropy change is derived from the magnetization measurements by using the Maxwell relation.

III. RESULTS

A. Crystal structure and phase transition

To properly evaluate the thermodynamic properties and enable comparison with results on other materials, it is essential to properly characterize the composition, homogeneity, and characteristics of the combined magnetic and structural phase transition. Neutron diffraction measurements were therefore carried out on $\text{Mn}_{1.1}\text{Fe}_{0.9}\text{P}_{0.76}\text{Ge}_{0.24}$ to determine the changes of the crystal and magnetic structures that occur during the first order transition induced by temperature or magnetic field, and the powder-diffraction patterns at 295 K and at 13 K were shown in Figs. 1(a) and 1(b), respectively. The data collected at 295 K and 13 K showed that the main phase of the sample is fully paramagnetic and ferromagnetic, respectively, at these temperatures. The refinements were performed using the Fe_2P -type hexagonal $P\bar{6}2m$ space group for the nuclear structure and a $P11m'$ symmetry for the magnetic structure. As shown in Fig. 2 and presented in Table I, the 3g pyramidal sites are occupied exclusively by Mn and the Fe/Mn atoms are located at the 3f tetrahedral sites. The intra-plane transition metals form a triangular configuration. The ferromagnetic Mn and Fe/Mn moments were found to lie in the a - b plane.

Fig. 3 shows the effect of temperature on the PM-FM transition. The well resolved (001) reflections of the PM and FM phases shown in the inset of Fig. 3(a) indicates that the two phases are structurally distinct. The integrated intensity of the (001) reflections for the PM and FM phases measured on cooling, at a speed of 10 K/h, is shown in Fig. 3(a) and indicates a first order phase transition. The sample is in the

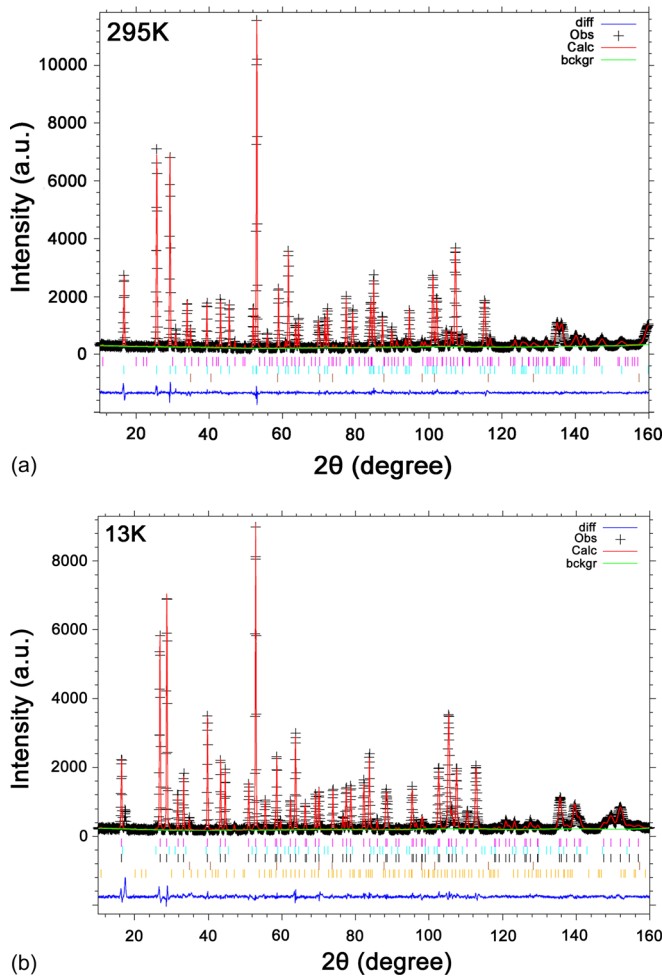


FIG. 1. Neutron powder-diffraction patterns of $\text{Mn}_{1.1}\text{Fe}_{0.9}\text{P}_{0.76}\text{Ge}_{0.24}$ at 295 K (a) and at 13 K (b).

fully paramagnetic state above ~ 272 K, while the PM and FM phases coexist below this temperature. It is observed [Fig. 3(b)] that $\sim 85.5\%$ of the sample transforms quickly between 272 and 263 K, but the rest of the sample remains in the paramagnetic state and continues to transform into the FM phase only very slowly with decreasing temperature. Eventually the entire sample has transformed.

Figure 4 shows the effect of an applied magnetic field on the PM-FM transition. The integrated intensity of the (001) reflections for the PM and FM phases as a function of the magnitude of the magnetic field are shown in Fig. 4(a),

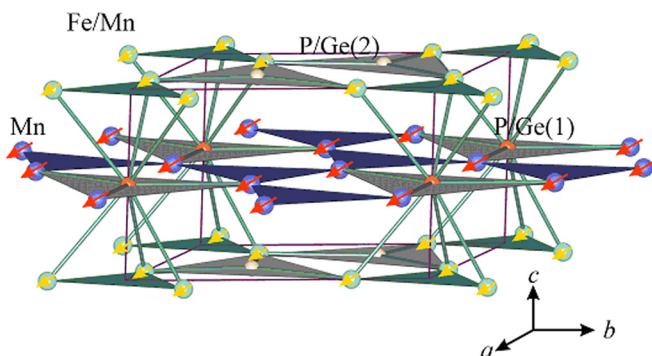


FIG. 2. Crystal and magnetic structures of $\text{Mn}_{1.1}\text{Fe}_{0.9}\text{P}_{0.76}\text{Ge}_{0.24}$ in the ferromagnetic state.

TABLE I. Structural parameters of $\text{Mn}_{1.1}\text{Fe}_{0.9}\text{P}_{0.76}\text{Ge}_{0.24}$ at 295 K and 13 K in zero field. Space group $P62m$. Atomic positions: Mn: $3g(x, 0, 1/2)$; Fe/Mn: $3f(x, 0, 0)$; P/Ge: $1b(0, 0, 1/2)$; P/Ge: $2c(1/3, 2/3, 0)$. Moments for Mn and Fe are restricted to the a - b plane and were then fixed along the a axis in the refinements.

		295 K	13 K
Parameters		PMP	FMP
Phase Fraction		100%	100%
a (Å)		6.06932(5)	6.19080(6)
c (Å)		3.45731(4)	3.30524(5)
V (Å ³)		110.294(2)	109.705(2)
Mn	x	0.5918(3)	0.5963(4)
	B (Å ²)	0.61(2)	0.33(6)
	M (μ_B)		3.89(7)
	$n(\text{Mn/Fe})$	0.973/0.027(3)	0.985/0.015(4)
Fe/Mn	x	0.2526(1)	0.2554(1)
	B (Å ²)	0.82(4)	0.34(2)
	M (μ_B)		1.38(8)
P/Ge(1)	$n(\text{Fe/Mn})$	0.923/0.077(5)	0.921/0.079(3)
	B (Å ²)	0.51(3)	0.26(6)
P/Ge(2)	$n(\text{P/Ge})$	0.976/0.024	0.93/0.07(2)
	B (Å ²)	0.68(3)	0.18(4)
$n(\text{P/Ge})$		0.751/0.249	0.74/0.26(2)
R_p (%)		4.20	5.25
wR_p (%)		5.39	7.2
χ^2		1.444	2.101

for a temperature of 272 K. At this temperature, most of the PM phase transforms to the FM phase between 1.4 T and 4.1 T, while the rest continues to transform slowly at higher magnetic fields. Fig. 4(b) shows that the transition is not completed even at 7 T, with about 17% of the sample remaining in the paramagnetic state. The behavior of the transition with field is quite similar to that the temperature dependence illustrated in Fig. 3 and will be interpreted in the following discussion.

To shed light on the nature of the crystal structures of both the PM and FM phases and how they evolve as a function of temperature and magnetic field, high-resolution neutron powder diffraction data were collected with high statistical accuracy at four temperature-field values, 267 K/0 T, 259 K/0 T, 271 K/3 T, and 271 K/6.9 T, where the PM and FM phases coexist (Figs. 3 and 4). The refinements reveal the detailed structures for both phases, and are given in Table II. The crystal structure evolution during the transition exhibits similar behavior in all four cases, namely, the lattice parameter a increases and lattice parameter c decreases substantially, while the cell volume remains nearly constant. The variations of the lattice parameters are shown in Table III. It is interesting to note that the atomic occupancies in both the PM and FM phases at 259 K/0 T is, within uncertainties, the same as that of the data at 271 K/3 T. Considering that all the parameters in the two sets of data are very similar, it is clear that they undergo almost identical crystal structural evolutions when the transition is driven by either the temperature or the magnetic field. The magnetic moment per formula unit $M_{f.u.}$ ($M_{f.u.} = M_{\text{Mn}} + M_{\text{Fe}}$) of Mn and Fe is constant ($\sim 4.1(1) \mu_B$) for the data at 267 K/0 T, 259 K/0 T, and 271 K/3 T but

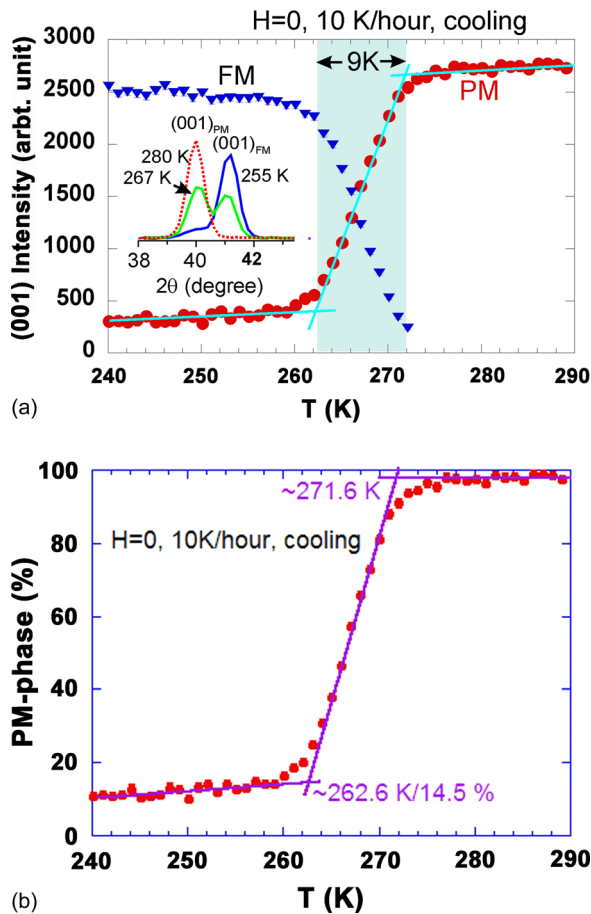


FIG. 3. (a) Integrated intensities of the (001) reflections of the PM and FM phases measured on cooling at a speed of 10 K/h. Inset: (001) peak(s) above (280 K), at (267 K), and below (255 K) the PM-FM transition. Note that the change in the a lattice parameter between the PM and FM phases is more than sufficient to separate the (001) peaks. (b) PM phase fraction as a function of temperature. About 85.5% of the paramagnetic phase transforms to the ferromagnetic phase in the temperature interval from 272 to 263 K, while the remaining 14.5% changes only very slowly below 263 K with further decrease of temperature.

increases by 15% to $4.7(1) \mu_B$ at 6.9 T and 271 K. Without an applied magnetic field, the Mn moments are 3 times larger than those of Fe, and both moments increase with the decreasing temperature, which agrees well with our previous investigations of the $Mn_{1.1}Fe_{0.9}P_{0.8}Ge_{0.2}$ compound.^{12,15}

To further elucidate the nature of the crystal structure evolution in the transition as a function of temperature or magnetic field, selected inter-atomic distances and angles at 267 K/0 T, 259 K/0 T, 271 K/3 T, and 271 K/6.9 T are provided in Table IV. It is observed that in all four cases the intra-layer metal-metal bond distances show a remarkable increase, while the inter-layer distances either remain constant or decrease slightly, during the PM \rightarrow FM transition. Further analyses indicate that the increase of the a - b axes lattice parameter is mainly due to the significant increase of intra-layer metal-metal bond distances and the shortening of the c -axis is mainly caused by a decrease of the P/Ge(1)-Fe/Mn-P/Ge(1) angle ($\sim 3\%$). It is, therefore, concluded that the transition from the PM to FM phase in the $Mn_{1.1}Fe_{0.9}P_{0.76}Ge_{0.24}$ compound induced by either temperature or magnetic field exhibits identical crystal structure evolution.

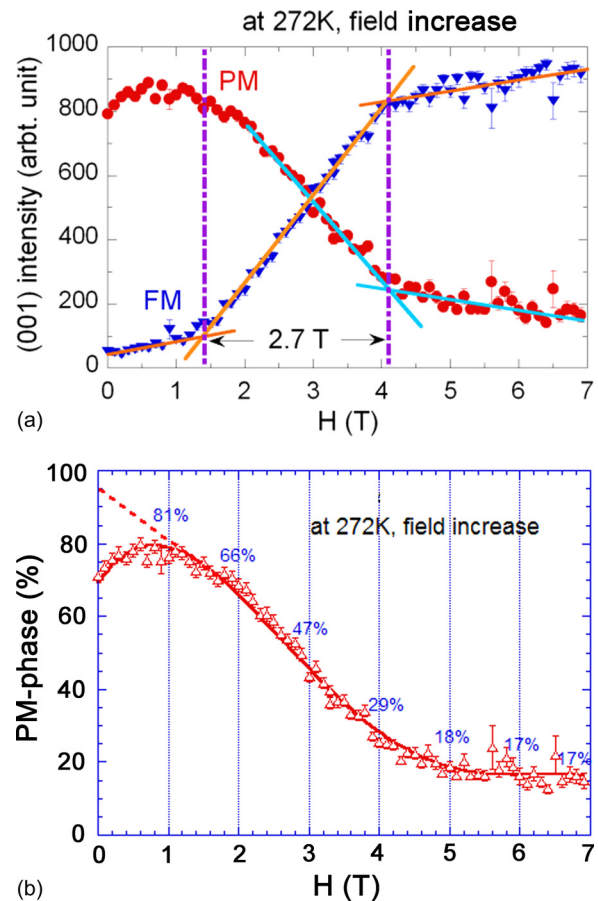


FIG. 4. (a) Field dependence of the integrated intensities of the (001) neutron reflections for the PM and FM phase at 272 K, (b) PM phase fraction as a function of magnetic field. About 82% of the paramagnetic phase changes quickly to the ferromagnetic phase from 0 to 5 T, while the remaining 18% changes only slowly with increased magnetic field.

The results of tables II–IV show that in FM phase bond distances, magnetic moments, lattice parameters and FM phase fraction in the sample are almost the same at 259 K/0 T and 271 K/3 T, although they are of course significantly different from the corresponding ones in the PM phase. Therefore, that the entropy changes are also approximately the same in the two cases.

B. DSC results

DSC is an appropriate method to study the thermal properties of a first order phase transitions since it provides a reliable and quantitative way to measure the transition temperature, thermal hysteresis, latent heat, and entropy changes associated with the transition. Fig. 5 shows the temperature dependence of the entropy in rates of 60 K/h or 300 K/h upon cooling and warming. It is observed that the rate of temperature change only slightly affects the entropy but does not alter the transition temperature range. The transition started at 271 K and ended at 261 K under cooling (Fig. 5(a)), and started at 282 K and ended at 273 K under warming (Fig. 5(b)), indicating a ~ 11 K thermal hysteresis. For comparison, the phase fraction shown in Fig. 3(a) is also plotted in Fig. 5(a) to reveal that neutron diffraction and DSC measurements give an identical temperature breadth of ~ 10 K upon cooling, and confirmed that the entropy change is

TABLE II. Structural parameters of $\text{Mn}_{1.1}\text{Fe}_{0.9}\text{P}_{0.76}\text{Ge}_{0.24}$ at 267 K/0 T, 259 K/0 T, 271 K/3 T, and 271 K/6.9 T. Space group $P\bar{6}2m$. Atomic positions: Mn: $3g(x, 0, 1/2)$; Fe/Mn: $3f(x, 0, 0)$; P/Ge: $1b(0, 0, 1/2)$; P/Ge: $2c(1/3, 2/3, 0)$. Moments for Mn and Fe were set parallel to the a direction (equivalent to the a - b plane for a powder) in the refinements.

Parameters	267 K/0 T		259 K/0 T		271 K/3 T		271 K/6.9 T	
	PMP	FMP	PMP	FMP	PMP	FMP	PMP	FMP
Phase Fraction	43.1%	52.3%	14.2%	81.7%	16.6%	79.9%	11.3%	85.3%
a (Å)	6.0818(1)	6.15584(7)	6.0799(6)	6.15891(6)	6.0775(5)	6.15511(8)	6.087(1)	6.15520(9)
c (Å)	3.4466(1)	3.36402(7)	3.4463(5)	3.35934(6)	3.4505(5)	3.3652(1)	3.439(1)	3.36090(8)
V (Å ³)	110.402(3)	110.399(3)	110.32(2)	110.355(3)	110.37(2)	110.41(2)	110.37(4)	110.274(4)
Mn								
x	0.5929(5)	0.5965(4)	0.594137	0.5961(4)	0.5941	0.5943(6)	0.5941	0.5941(5)
B (Å ²)		0.64(2)		0.11(6)		0.49(6)		0.40(5)
M (μ_B)		3.02(8)		3.49(7)		3.4(1)		4.1(7)
n(Mn/Fe)	0.997/0.003(2)	0.996/0.004(3)	0.991/0.009	0.974/0.026(4)	0.991/0.009	0.974/0.026	0.991/0.009	0.977/0.023
Fe/Mn								
x	0.2536(2)	0.2543(2)	0.254921	0.2543(1)	0.2549	0.2550(2)	0.2549	0.2546(2)
B (Å ²)		0.64(2)		0.57(2)		0.92(3)		0.74(3)
M (μ_B)		1.06(9)		0.71(8)		0.6(1)		0.63(7)
n(Fe/Mn)	0.931/0.069(3)	0.943/0.057(3)	0.939/0.061	0.95/0.05	0.939/0.061	0.95/0.05	0.939/0.061	0.937/0.063
P/Ge(1)								
B (Å ²)		0.44(4)		0.66(6)		1.00(6)		0.79(5)
n(P/Ge)	0.89/0.11(2)	0.90/0.11(2)	0.906/0.094	0.78/0.22(2)	0.906/0.094	0.78/0.22	0.906/0.094	0.810/0.190
P/Ge(2)								
B (Å ²)		0.44(4)		0.33(4)		0.63(4)		0.57(4)
n(P/Ge)	0.69/0.31(2)	0.71/0.29(2)	0.712/0.288	0.68/0.32(2)	0.712/0.288	0.681/0.319	0.712/0.288	0.672/0.328
R_p (%)		3.94		4.66		8.11		6.78
wR_p (%)		5.12		6.08		10.03		8.53
χ^2		2.51		3.358		2.136		1.602

TABLE III. Lattice parameter variations from the PM phase to the FM phase in $\text{Mn}_{1.1}\text{Fe}_{0.9}\text{P}_{0.76}\text{Ge}_{0.24}$ at 267 K/0 T, 259 K/0 T, 271 K/3 T, and 271 K/6.9 T.

Parameters	267 K/0 T	259 K/0 T	271 K/3 T	271 K/6.9 T
Δa (%)	+1.2174	+1.2995	+1.277	+ 1.1204
Δc (%)	-2.396	-2.5233	-2.4721	-2.271
ΔV (%)	-0.0027	+0.0317	+0.03624	-0.08698
$\Delta(c/a)$ (%) ^a	3.5	4.2	3.7	3.3

^a $\Delta(c/a)$ is the c/a of PM phase at 295 K different from c/a of FM phase induced by temperature or magnetic field.

directly related to the FM phase fraction.^{12,15} The average integrated entropy changes from 240 K to 300 K upon cooling and from 261 K to 300 K upon warming are 33.81 and 30.76 J/kg·K, respectively. Note that only 81.7% of the PM phase was converted into FM at 259 K, and there is still $\sim 4\%$ MnO impurity in the sample. Hence average entropy changes as high as 42.71 J/kg·K could be achieved if the phase transformation goes to completion in a pure sample. From the DSC measurements, we obtained some very important parameters, i.e. (1) crystal and magnetic phase transition temperature; (2) thermal hysteresis of the transition;

TABLE IV. Selected inter-atomic distances (Å) and angles (degree) of the PM and FM phases in $\text{Mn}_{1.1}\text{Fe}_{0.9}\text{P}_{0.76}\text{Ge}_{0.24}$ at 267 K/0 T, 259 K/0 T, 271 K/3 T, and 271 K/6.9 T.

	267 K/0 T		259 K/0 T		271 K/3 T		271 K/6.9 T	
	PMP	FMP	PMP	FMP	PMP	FMP	PMP	FMP
	Intra plane metal to metal distance							
Mn-Mn	3.195(2)	3.245(2)	3.197(6)	3.245(1)	3.196(3)	3.238(2)	3.202(1)	3.237(2)
Fe/Mn-Fe/Mn	2.672(3)	2.711(2)	2.6845(2)	2.713(2)	2.6835(2)	2.719(3)	2.68796(6)	2.7146(2)
	Inter plane metal to metal distance							
Mn- Fe/Mn	2.689(3)	2.696(2)	2.6875(2)	2.693(2)	2.6882(2)	2.683(3)	2.6871(5)	2.682(3)
Mn- Fe/Mn	2.768(2)	2.750(2)	2.7633(2)	2.751(1)	2.7640(2)	2.758(2)	2.7632(5)	2.758(2)
	Fe/MnP4 tetrahedron distance							
Fe/Mn-P/Ge(2) $\times 2$	2.3082(9)	2.3336(7)	2.3023(2)	2.3346(6)	2.3014(2)	2.3304(9)	2.3052(5)	2.3320(8)
Fe/Mn-P/Ge(1) $\times 2$	2.313(1)	2.2977(7)	2.3176(2)	2.2968(6)	2.3188(2)	2.301(1)	2.3162(5)	2.2978(8)
	MnP5 pyramid distance							
Mn-P/Ge(1)	2.476(3)	2.484(3)	2.4676(2)	2.487(2)	2.4667(2)	2.496(4)	2.4707(6)	2.498(3)
Mn-P/Ge(2) $\times 4$	2.5242(7)	2.5180(6)	2.5253(2)	2.5165(5)	2.5262(2)	2.5152(9)	2.5245(5)	2.5134(7)
	Intra plane angle							
P/Ge(1)-Fe/Mn-PGe(1)	96.34(5)	94.00(4)	96.06(1)	94.00(3)	96.15(1)	93.98(5)	95.87(2)	93.99(4)
P/Ge(2)-Fe/Mn-PGe(2)	99.04(5)	99.19(4)	99.339(0)	99.21(3)	99.399(0)	99.36(5)	99.339(0)	99.27(4)

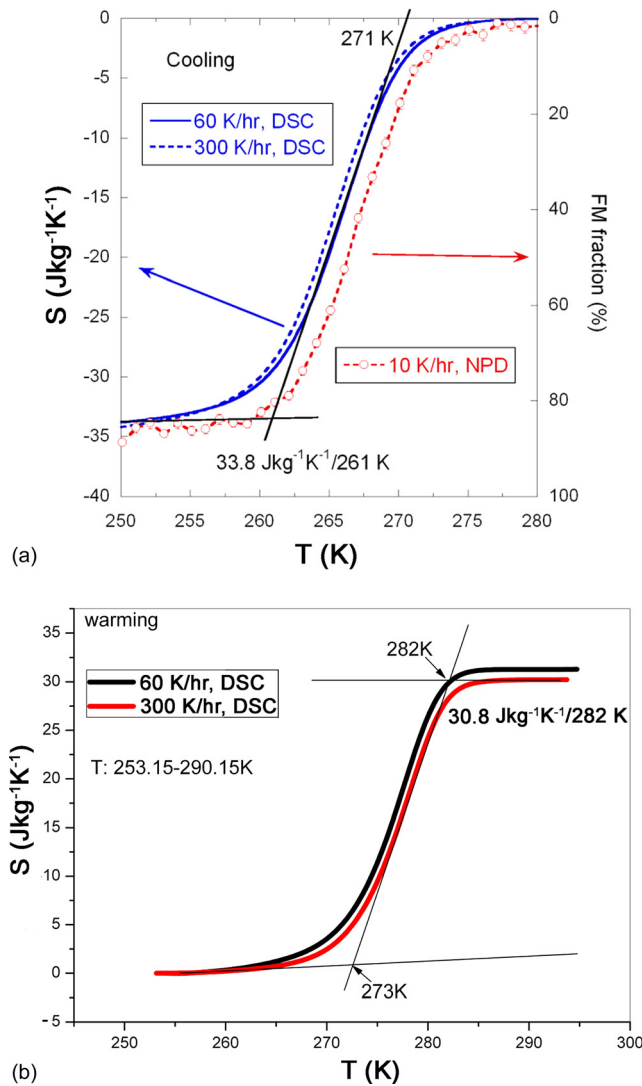


FIG. 5. PM-FM phases transformation entropy of $\text{Mn}_{1.1}\text{Fe}_{0.9}\text{P}_{0.76}\text{Ge}_{0.24}$ as a function of temperature calculated from DSC data, in rates of 1 K/min or 5 K/min. (a) cooling, with $\Delta S = 33.8 \text{ J/kg K}$, and (b) warming, with $\Delta S = 30.8 \text{ J/kg K}$.

(3) temperature range of the two-phase coexistence; and (4) both the structural and magnetic entropy change of the transition of the sample, and estimated maximum entropy change of the transition for a pure and totally transformed compound when combined with the nuclear and magnetic structure analysis. These results are important because they indicate that the measured ΔS by means of the DSC method, where the transition is temperature induced, is also valid to a good approximation when the transition is field-induced. This allows a reliable determination of ΔS using the DSC technique without magnetic measurements that are controversial, or in some case, incorrect.^{23,24} This is an advantage for those practical applications such as refrigeration that require the use of a magnetic field.

C. Magnetic measurements results

Fig. 6 Temperature dependence of the magnetic entropy change in bulk $\text{Mn}_{1.1}\text{Fe}_{0.9}\text{P}_{0.76}\text{Ge}_{0.24}$ as a function of magnetic field up to 5 T determined using the Maxwell relation. The steps of temperature and magnetic field used in the measurements were 1 K and 0.1 T.

The temperature dependence of the magnetic entropy change ΔS_M shown in Fig. 6 was obtained using magnetization curves and the Maxwell relation. The measurements were made under four conditions: (i) increasing temperature-increasing field; (ii) increasing temperature-decreasing field; (iii) decreasing temperature-increasing field; (iv) decreasing temperature-decreasing field. All the curves show similar shapes. Note in particular that the differences reported in Refs. 25 and 26 from the different measuring methods are not found in our results. Note also that the transition temperatures shown in Fig. 6 are consistent with those obtained from the neutron diffraction and DSC measurements. The results from the four types of measurements give similar values of ΔS_M . The height of the peaks increases with increasing magnetic field due to an increase of the FM phase fraction. However, it is still need to mention that the four

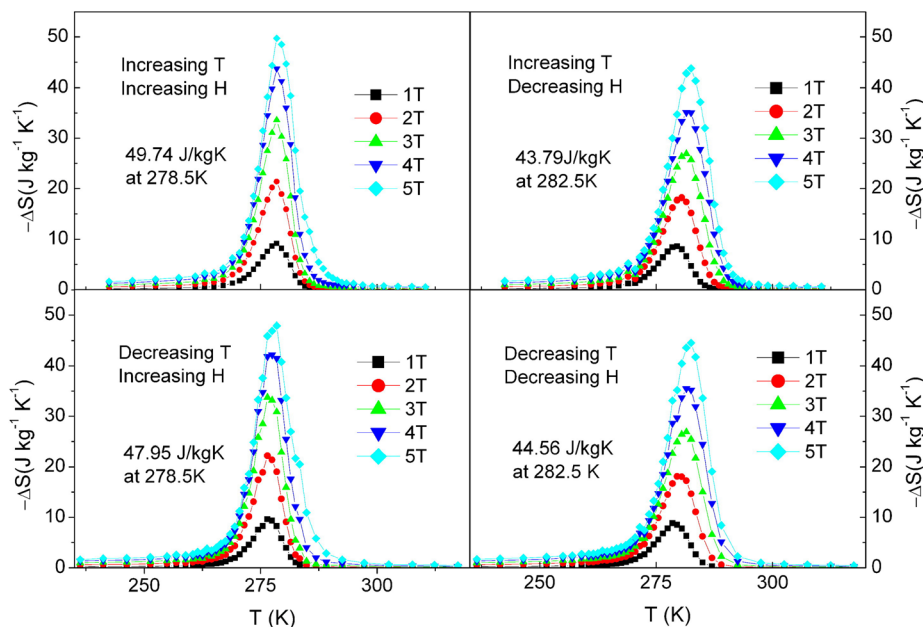


FIG. 6. Temperature dependence of the magnetic entropy change in bulk $\text{Mn}_{1.1}\text{Fe}_{0.9}\text{P}_{0.76}\text{Ge}_{0.24}$ as a function of magnetic field up to 5 T determined using the Maxwell relation. The steps of temperature and magnetic field used in the measurements were 1 K and 0.1 T.

types of measurements result different magnetic transition process in the alloy, so we find an average ΔS_M value of 46.5 J/kg·K for fields from 0 to 5 T for this sample, which translates to maximum value of 58.1 J/kg·K after correction for the impurity and phase fraction. We note that these values are substantially larger than the measured $\Delta S_{DSC} = 33.8$ J/kg·K and maximum ideal value of 42.7 J/kg·K for an impurity-free and completely homogeneous sample, obtained directly from the DSC technique.

IV. DISCUSSION

The results discussed in the previous sections unambiguously show that the magnetic and structural transitions in $Mn_{1.1}Fe_{0.9}P_{0.76}Ge_{0.24}$ induced by temperature are almost identical to the transitions induced by the application of a magnetic field. This consideration is based on the comparison between the FM phase parameters reported in Tables II–IV for the experiments done at 259 K/0 T and 271 K/3 T, where phase fractions, lattice parameters, magnetic moments, occupancy factors and bond distances and angles, do not differ from each other by more than 1–2 times of the standard deviations. As noted previously, under these conditions, it is expected that the entropy changes are also approximately the same in the two cases. This conclusion suggests that the measured ΔS by means of the DSC method, where the transition is temperature induced, is also valid when the transition is induced by a magnetic field (which is usually the case in technological applications).

A comparison of the values of ΔS (and MCE) obtained with the DSC method and those derived from the magnetization curves and the Maxwell equation, in the same or in closely related compounds, shows that in some cases there are substantial differences. More specifically, the values of the entropy changes obtained from magnetization measurements can be either larger or smaller than those obtained with the DSC method, depending on the range of the transition temperature as well as the magnitude of the applied field. Moreover, the differences between ΔS_M and ΔS may be due to the contributions from the structural transition and magnetic order having the same or opposite signs. In addition, a large body of research^{6,9,14,25} has shown that the use of magnetic measurements to derive ΔS is controversial and, in some cases, clearly incorrect. This is especially true in the vicinity of T_c for first order transitions.^{25–27} We therefore conclude that detailed comparisons are only reliable using the DSC technique, on well characterized samples where the structures and phase fractions are known.

V. CONCLUSIONS

In conclusion, the transition processes from the PM to FM phase in the $Mn_{1.1}Fe_{0.9}P_{0.76}Ge_{0.24}$ compound induced by both temperature and by magnetic field show similar behavior, with the two processes undergoing identical crystal and magnetic structure changes. This supports the conclusion that reliable entropy changes and other important thermodynamic properties associated the transitions can be obtained by DSC measurements combined with the structure and magnetic properties (magnetic moments, bond distances, distortions, etc.) of the

materials being investigated. The large measured entropy change of 33.8 J kg⁻¹ K⁻¹ near T_c for our sample could be improved to a value as high as 42.71 J kg⁻¹ K⁻¹ for a pure, homogeneous $Mn_{1.1}Fe_{0.9}P_{0.76}Ge_{0.24}$ compound with complete PM → FM phase transformation. Our results indicate that this material has good potential for magnetic refrigeration applications.

ACKNOWLEDGMENTS

The work was supported by the Beijing Natural Science Foundation (1112005), the National Natural Science Foundation of China (51171003, 51071007) and the National Basic Research Program of China (2010CB8331001). The identification of any commercial product or trade name does not imply endorsement or recommendation by the National Institute of Standards and Technology.

- ¹J. Glanz, *Science* **279**, 2045 (1998).
- ²K. V. Pecharsky and K. A. Gschneidner, *Phys. Rev. Lett.* **78**, 4494 (1997).
- ³F. X. Hu, B. G. Shen, J. R. Sun, and Z. H. Cheng, *Appl. Phys. Lett.* **78**, 3675 (2001).
- ⁴O. Tegus, E. Brück, K. H. J. Buschow, and F. R. de Boer, *Nature* **415**, 150 (2002).
- ⁵F. X. Hu, B. G. Shen, and J. R. Sun, *Appl. Phys. Lett.* **76**, 3460 (2000).
- ⁶W. Dagula, O. Tegus, B. Fuquan, L. Zhang, P. Z. Si, M. Zhang, W. S. Zhang, E. Brück, F. R. de Boer, and K. H. J. Buschow, *IEEE Trans. Magn.* **41**, 2778 (2005).
- ⁷Z. Q. Ou, G. F. Wang, S. Lin, O. Tegus, E. Brück, and K. H. J. Buschow, *J. Phys: Condens Matter.* **18**, 11577 (2006).
- ⁸D. T. Cam Thanh, E. Brück, O. Tegus, J. C. P. Klaasse, T. J. Gortenmulder, and K. H. J. Buschow, *J. Appl. Phys.* **99**, 08Q107 (2006).
- ⁹A. Yan, K. H. Müller, L. Schultz, and O. Gutfleisch, *J. Appl. Phys.* **99**, 08K903 (2006).
- ¹⁰M. T. Sougrati, R. P. Hermann, F. Grandjean, G. J. Long, E. Brück, O. Tegus, N. T. Trung, and K. H. J. Buschow, *J. Phys: Condens Matter.* **20**, 475206 (2008).
- ¹¹X. B. Liu, Z. Altounian, D. H. Ryan, M. Yue, Z. Q. Li, D. M. Liu, and J. X. Zhang, *J. Appl. Phys.* **105**, 07A920 (2009).
- ¹²D. M. Liu, M. Yue, J. X. Zhang, T. M. McQueen, J. W. Lynn, X. L. Wang, Y. Chen, J. Y. Li, R. J. Cava, X. B. Liu, Z. Altounian, and Q. Huang, *Phys. Rev. B* **79**, 014435 (2009).
- ¹³M. Yue, Z. Q. Li, X. L. Wang, D. M. Liu, J. X. Zhang, and X. B. Liu, *J. Appl. Phys.* **105**, 07A915 (2009).
- ¹⁴N. T. Trung, Z. Q. Ou, T. J. Gortenmulder, O. Tegus, K. H. J. Buschow, and E. Brück, *Appl. Phys. Lett.* **94**, 102513 (2009).
- ¹⁵D. M. Liu, Q. Huang, M. Yue, J. W. Lynn, L. J. Liu, Y. Chen, Z. H. Wu, and J. X. Zhang, *Phys. Rev. B* **80**, 174415 (2009).
- ¹⁶M. Yue, Z. Q. Li, X. B. Liu, H. Xu, D. M. Liu, and J. X. Zhang, *J. Alloys Compd.* **493**, 22 (2010).
- ¹⁷M. Yue, Z. Q. Li, H. Xu, Q. Z. Huang, X. B. Liu, D. M. Liu, and J. X. Zhang, *J. Appl. Phys.* **107**, 09A939 (2010).
- ¹⁸V. K. Pecharsky and K. A. Gschneidner, *J. Appl. Phys.* **86**, 565 (1999).
- ¹⁹A. Giguère, M. Foldeaki, B. Ravi Gopal, R. Chahine, T. K. Bose, A. Frydman, and J. A. Barclay, *Phys. Rev. Lett.* **83**, 2262 (1999).
- ²⁰J. Marcos, F. Casanova, X. Batlle, A. Labarta, A. Planes, and L. Mañosa, *Rev. Sci. Instrum.* **74**, 4768 (2003).
- ²¹M. Kuepferling, C. P. Sasso, V. Basso, and L. Giudici, *IEEE Trans. Magn.* **43**, 2764 (2007).
- ²²S. Jeppesen, S. Linderoth, N. Pryds, L. Thei Kuhn, and J. Buch Jensen, *Rev. Sci. Instrum.* **79**, 083901 (2008).
- ²³S. Gama, A. A. Coelho, A. de Campos, A. M. G. Carvalho, F. C. G. Gandra, P. J. von Ranke, and N. A. de Oliveira, *Phys. Rev. Lett.* **93**, 237202 (2004).
- ²⁴C. Xu, G. D. Li, and L. G. Wang, *J. Appl. Phys.* **99**, 123913 (2006).
- ²⁵L. Caron, Z. Q. Ou, T. T. Nguyen, D. T. Cam Thanh, O. Tegus, and E. Brück, *J. Magn. Magn. Mater.* **321**, 3559 (2009).
- ²⁶H. W. Zhang, J. Shen, Q. Y. Dong, T. Y. Zhao, Y. X. Li, J. R. Sun, and B. G. Shen, *J. Magn. Magn. Mater.* **320**, 1879 (2008).
- ²⁷G. J. Liu, J. R. Sun, J. Shen, B. Gao, H. W. Zhang, F. X. Hu, and B. G. Shen, *Appl. Phys. Lett.* **90**, 032507 (2007).